COBEM 2021 26th International Congress of Mechanical Engineering
November 22-26, 2021, Virtual Congress, Brazil

COB-2021-2333 SMART BEAM COUPLED TO PIEZOELECTRIC RESONANT SHUNT VIBRATION CHARACTERIZATION, CONTROL AND BANDGAP GENERATION

Braion B. Moura
Matheus C. R. Borges
Marcela R. Machado
Department of Mechanical Engineering, University of Brasília, University Campus Darcy Ribeiro, Faculty of Technology, Asa Norte, Brasília – DF, 70910900
braionbarbosa@gmail.com
canedo001@gmail.com
marcelam@unb.br

Abstract. *This paper analyses the dynamic behavior of a beam with piezoelectrics (piezos) coupled in a periodic array of resonant shunted patches in unimorph configuration. Based on the piezo ability to convert mechanical energy to electrical energy and vice versa, the connection of the resonant shunt circuit is adopted to provide vibration and wave propagation attenuation. Due to the piezo patches periodic array connected with a resonant shunt circuit, a vibration isolation band in a tuned frequency is expected. This effect is known as bandgap. Therefore, the results show the bandgap's effects and its characteristics relative to the unimorph piezoelectric configurations. The spectral elements method (SEM) is an efficient method requiring no discretization or a reduced number other than the element in the mesh element. Therefore, it is an efficient technique to analyses the structure's vibration response. The dispersion diagram is obtained using the transfer matrix method (TMM). The receptance response and the dispersion diagrams demonstrate the vibration and wave control effect by the resonant circuit, and also demonstrate the influence of the amount of piezos for the bandgap generation.*

Keywords: *Smart beam, Vibration control, Piezoelectric, Resonant Shunt, Bandgap.*

1. INTRODUCTION

The use of smart materials has increased in recent years due to the specific needs for certain systems' dynamic and acoustic properties. Many smart structures deal with the inclusion of piezoelectric materials (piezo) to monitor and control vibration. The control vibration with the piezo coupled in these smart structures is based on converting energy from the mechanical domain to the electrical domain and vice versa (Forward, 1979). The piezo is exposed to an electric field to produce a mechanical voltage, the effect of reverse piezoelectric occurs. When the piezo is exposed to a mechanical voltage to produce an electric field, the direct piezoelectric effect occurs. Vibration controls that use direct and reverse piezoelectric effects can be classified into passive, active and hybrid controls (Jaffe *et al*., 1971). The techniques of active vibration control are related to the reverse piezoelectric effect, where they use an electrical energy source to increase the mechanical energy needed by the system (Santana et al., 2003). Unlike active techniques, passive vibration control techniques use the direct piezoelectric effect, making changes in the electrical energy generated by the piezo to promote a specific dynamic property in the structure without depending on an external source of electrical energy. Hybrid controls combine active and passive control techniques.

In the literature, the passive vibration control is when piezo's are connected with external electrical circuits composed of passive components such as resistors, inductors and capacitors (Gripp and Rade, 2018). These passive electrical circuits are known as shunt circuits. Therefore, in this article, passive vibration control is addressed in a smart structure beam coupled with piezo's connected to a series resistive-inductive (RL) shunt electrical circuit. The piezo's are connected in periodic arrangements to promote a bandgap effect, a vibration isolation band effect on a tuned frequency (Chen *et al*., 2014).

Dynamic models of smart structures connected with circuits shunts are generally developed based on Modal Analysis (MA), Finite Element Method (FEM), Finite Wave Element (WFE), among other techniques (Leo, 2007). However, these methods require a certain mathematical complexity, and some need a large number of discretization's to express precision in the system's responses. The Spectral Element Method (SEM) is an alternative to other methods since its formulation deals with a model that relates forces and displacements spectral nodal based on the analytical solution of the wave (Doyle, 1997). Therefore, SEM does not need a discretization with large numbers of elements. Based on this context, this article discusses the development of an SEM numerical model of a unimorph beam structure, represented by a beam coupled with a piezo layer. Numerical modelling of the resistive-inductive resonant shunt circuit is also performed to connect it to the piezo's. The interactions between the structure and the shunt circuit are given by the general impedance relationships

of the circuit. The system modelling with more than one piezo coupled uses the Transfer Matrix Method (TMM) to allocate spectral dynamic stiffness matrices to join subdivisions of the structure and estimate the dispersion diagram. Based on this information, this work intends to continue the previous work published in (Barbosa and Machado, 2019; Machado *et al*., 2019; Moura, B. *et al*., 2020; and Moura and Machado, 2021).

2. SPECTRAL ELEMENT THEORY BACKGROUND

The smart beam structure model of Figure 1, used the piezo patched couplings in a periodical order. The periodicity influences the generation of the bandgap effect.

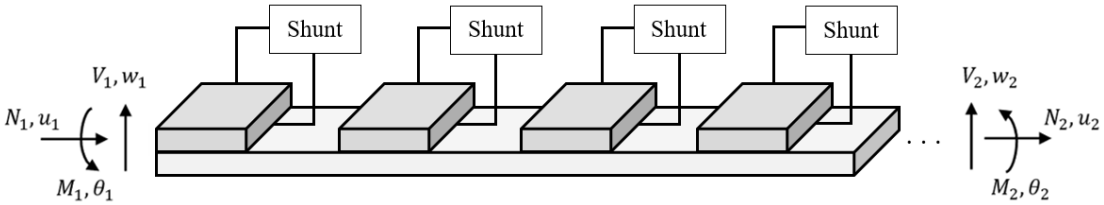

Figure 1. Smart material beam.

The smart beam represented in Figure 1 is composed of joints of elements of the type beam-piezo-shunt and beam classic. In both elements, the Euler-Bernoulli theory is adopted. The structure presents uniform density and thickness, perfect continuity at the interfaces, small vibration amplitudes and linear elasticity. The variables of transverse displacement, axial displacement and rotation are represented by the terms $w(x,t)$, $u(x,t)$ and $\theta(x,t)$. The relations of bending moments, shear force and axial force, are represented by M, V and N.

2.1 Beam spectral element

The beams are structural elements that have the dimension of the cross-section less than the total length. In general, the mathematical model for a classic Euler-Bernoulli beam considering the dimensions uniform prismatic has the following equation of motion,

$$EI\ \frac{\partial^4 w(x,t)}{\partial x^4} = \rho A \frac{\partial^2 \theta(x,t)}{\partial t^2} + f(x,t) \tag{1}$$

where E, ρ, A and I are Young's modulus, mass density, transverse area and moment of inertia, respectively. Assuming that the transverse displacement and rotation can be expressed as

$$\begin{Bmatrix} w(x,t) \\ \theta(x,t) \end{Bmatrix} = \frac{1}{N}\sum_{n=0}^{N-1} \begin{Bmatrix} W(x,\omega_n) \\ \Theta(x,\omega_n) \end{Bmatrix} e^{i\omega_n t} \tag{2}$$

By considering the external force $f(x,t) = 0$, and applying the spectral terms of Eq. (2) in Eq. (1), we obtained the equation of movement of beam in the frequency domain, expressed by

$$EI\ \frac{\partial^4 W(x,\omega_n)}{\partial x^4} - \omega^2 \rho A W(x,\omega_n) = 0 \tag{3}$$

Assuming a general solution of type $W = ae^{-ik(\omega)x}$ in Eq. (3), an eigenvalue problem is obtained, and its solution represents the following dispersion relation,

$$k^4 - k_F^4 = 0, \tag{4}$$

where k_F does the following relation define the wavenumber

$$k_F = \sqrt{\omega}\left(\frac{\rho A}{EI}\right)^{1/4} \tag{5}$$

With the obtained wavenumbers and the normalized eigenvectors, one can get the general solution

$$w = a_1 e^{-ik_F x} + a_2 e^{-k_F x} + a_3 e^{ik_F x} + a_4 e^{k_F x} = \boldsymbol{e}(x,\omega)\boldsymbol{a} \tag{6}$$

where

$$\boldsymbol{e}(x,\omega) = [e^{-ik_F x},\ e^{-k_F x},\ e^{ik_F x},\ e^{k_F x}], \qquad \boldsymbol{a} = \{a_1,\ a_2,\ a_3,\ a_4\}^{\boldsymbol{T}}$$

For finite beam element of length L with defined nodes on the contours $x = 0$ and $x = L$, we have that the transverse displacement and rotation can be related to the wave equation,

$$\boldsymbol{d} = \begin{Bmatrix} W_1 \\ \Theta_1 \\ W_2 \\ \Theta_2 \end{Bmatrix} = \begin{Bmatrix} \boldsymbol{e}(0,\omega) \\ \boldsymbol{e}'(0,\omega) \\ \boldsymbol{e}(L,\omega) \\ \boldsymbol{e}'(L,\omega) \end{Bmatrix} = \boldsymbol{H}_B(\omega)\boldsymbol{a}, \tag{7}$$

where

$$\boldsymbol{H}_B(\omega) = \begin{bmatrix} 1 & 1 & 1 & 1 \\ -ik_F & -k_F & ik_F & k_F \\ e^{-ik_F L} & e^{-k_F L} & e^{ik_F L} & e^{k_F L} \\ -ik_F e^{-ik_F L} & -k_F e^{-k_F L} & ik_F e^{ik_F L} & k_F e^{k_F L} \end{bmatrix},$$

Following the same logic as displacements, the components of force and moment can be expressed as

$$\boldsymbol{f_c} = \begin{Bmatrix} Q_1 \\ M_1 \\ Q_2 \\ M_2 \end{Bmatrix} = \begin{Bmatrix} -Q(0) \\ -M(0) \\ Q(L) \\ M(L) \end{Bmatrix} = \boldsymbol{G}_B(\omega)\boldsymbol{a}, \tag{8}$$

where

$$Q(x) = -EIW'''(x), \qquad M(x) = EIW''(x),$$

$$\boldsymbol{G}_B(\omega) = \begin{bmatrix} -ik_F^3 & ik_F^3 & k_F^3 & -k_F^3 \\ -ik_F^2 & ik_F^2 & k_F^2 & -k_F^2 \\ ik_F^3 e^{-ik_F L} & -ik_F^3 e^{ik_F L} & -k_F^3 e^{k_F L} & k_F^3 e^{-k_F L} \\ k_F^2 e^{-ik_F L} & -k_F^2 e^{ik_F L} & ik_F^2 e^{k_F L} & -ik_F^2 e^{-k_F L} \end{bmatrix},$$

By relating Eq. (7) with Eq. (8), it is possible to establish the relations between displacement and force,

$$\boldsymbol{S}_B(\omega) = \boldsymbol{G}_B(\omega)\boldsymbol{H}_B^{-1}(\omega), \tag{9}$$

where $\boldsymbol{S}_B(\omega)$ is the dynamic stiffness matrix, also known as the spectral stiffness matrix for the Euler-Bernoulli beam.

2.2 Spectral element of beam-piezo

The linear constitutive relationships used to represent electromechanical behavior one-dimension of the piezoelectric material are expressed with,

$$\begin{Bmatrix} \sigma \\ E_c \end{Bmatrix} = \begin{bmatrix} C_{11}^D & -h_{31} \\ -h_{31} & \beta_{33}^S \end{bmatrix} \begin{Bmatrix} \epsilon \\ D_3 \end{Bmatrix}, \tag{10}$$

where σ is the mechanical stress, ϵ the mechanical strain, D_3 is the electrical displacement (charge/area in the vertical beam direction), β_{33}^S the dielectric constant, C_{11}^D is the elastic modulus, E_c is the dielectric constant, and h_{31} is the piezoelectric constant. The formulation of the spectral element starts with the exact solution of the equation of the motion. Therefore, to build the motion equation of a piezo coupled beam element, Lee (2009) uses the relations of kinetic energy, potential and virtual work to apply Hamilton's principle and generate the following motion of equation,

$$\begin{aligned} &EIw'''' + \rho A\ddot{w} + cA\dot{w} = -\alpha\ddot{u}_b' + \beta u''' + \gamma\ddot{w}'' + c_1\dot{w}'' - c_4\dot{u}_b' + Fw'' + p(x,t) \\ &EAu_b'' - \rho A\ddot{u}_b - cA\dot{u}_b = -\alpha\ddot{w}' + \beta w''' - c_4\dot{w}' - \tau(x,t), \end{aligned} \tag{11}$$

where

$$EA = E_bA_b + E_pA_p, \quad EI = E_bI_b + E_pI_p + (1/4)E_pA_ph^2, \quad c_1 = (1/4)c_pA_ph^2,$$
$$\rho A = \rho_bA_b + \rho_pA_p, \quad \alpha = (1/2)\rho_pA_ph, \quad c_4 = (1/2)c_pA_ph,$$
$$\beta = (1/2)E_pA_ph, \quad \gamma = (1/4)\rho_pA_ph^2, \quad cA = c_bA_b + c_pA_p,$$

where subscripts b e p represent the beam and piezo elements, respectively, the terms E, ρ, c, A and I are Young's modulus, mass density, viscous damping coefficient, transverse area and moment of inertia, respectively. The sum of the thicknesses of the beam and the piezo is represented by h; F is the constant axial tensile force, $p(x,t)$ and $\tau(x,t)$ are possible external forces applied along the beam. For simplification of notation, spatial partial derivatives are represented by ($'$), while partial time derivatives are characterized by ($\dot{}$).

The structural damping of each element can be readily taken into account using the complex modulus of elasticity as

$$E_b^* = E_b(1 + i\eta_b), \quad E_p^* = C_{11}^{D*} - h_{31}^2\beta_{33}^{S-1}, \quad C_{11}^{D*} = C_{11}^D(1 + i\eta_p) \tag{12}$$

The following spectral forms are assumed

$$\begin{Bmatrix} w(x,t) \\ u(x,t) \\ p(x,t) \\ \tau(x,t) \end{Bmatrix} = \frac{1}{N}\sum_{n=0}^{N-1} \begin{Bmatrix} W(x,\omega_n) \\ U(x,\omega_n) \\ P(x,\omega_n) \\ T(x,\omega_n) \end{Bmatrix} \tag{13}$$

Applying the spectral terms of Eq. (13) in Eq. (11), we obtained the equation of motion in the frequency domain, expressed by

$$\begin{aligned} &EIW'''' - \omega^2\rho AW + i\omega cAW = \omega^2\alpha U' + \beta U''' - \omega^2\gamma W'' + i\omega c_1W'' - i\omega c_4U' + FW'' + P(x) \\ &EAU'' + \omega^2\rho AU - i\omega cAU = \omega^2\alpha W' + \beta W''' - i\omega c_4W' - T(x), \end{aligned} \tag{14}$$

The general solution is assumed of type

$$\begin{aligned} W(x) &= \sum_{i=1}^{6}(a_je^{-ik_jx}) = \boldsymbol{e}(x,\omega)\boldsymbol{a} \\ U(x) &= \sum_{i=1}^{6}(r_ja_je^{-ik_jx}) = \boldsymbol{e}(x,\omega)\boldsymbol{R}\boldsymbol{a} \end{aligned} \tag{15}$$

where

$$\boldsymbol{e}(x,\omega) = [e^{-ik_1x} \;\; e^{-ik_2x} \;\; e^{-ik_3x} \;\; e^{-ik_4x} \;\; e^{-ik_5x} \;\; e^{-ik_6x}], \quad \boldsymbol{a} = \{a_1 \;\; a_2 \;\; a_3 \;\; a_4 \;\; a_5 \;\; a_6\}^T$$
$$\boldsymbol{R} = diag(r_j) = diag\left[\frac{-\omega k_jc_4 - i\omega^{2k_j}\alpha + ik_j^3\beta}{-k_j^2EA + \omega^2\rho A - i\omega cA}\right]$$

From the general solution applied to the equation of motion, a characteristic equation with an eigenvalue problem is obtained, and the wavenumbers k_j ($j = 1,2..,6$) are determined by estimating the roots of the following expression

$$x_1k^6 + x_2k^4 + x_3k^2 + x_4 = 0, \tag{16}$$

where

$$\begin{aligned} x_1 &= \beta^2 - EAEI, \\ x_2 &= \omega^2(EA\gamma + EI\rho A - 2\alpha\beta) - i\omega(EIcA + EAc_1 - 2\beta c_4) - EAF, \\ x_3 &= \omega^4(\alpha^2 - \gamma\rho A) + i\omega^3(\rho Ac_1 + \gamma cA - 2\alpha c_4) + \omega^2(EA\rho A + cAc_1 + F\rho A - c_4^2) - i\omega cA(EA + F), \\ x_4 &= -\rho A^2\omega^4 + 2i\omega^3\rho AcA + \omega^2cA^2. \end{aligned}$$

Relating the spectral nodal shifts in terms of $\boldsymbol{a}$ with the vector $\boldsymbol{d}$, we obtain

$$\boldsymbol{d} = \boldsymbol{H}_{BP}(\omega)\boldsymbol{a}, \tag{17}$$

where

$$\boldsymbol{H}_{BP}(\omega)=\begin{bmatrix} r_1 & r_2 & r_3 & r_4 & r_5 & r_6 \\ 1 & 1 & 1 & 1 & 1 & 1 \\ -ik_1 & -ik_2 & -ik_3 & -ik_4 & -ik_5 & -ik_6 \\ e^{-ik_1L}r_1 & e^{-ik_2L}r_2 & e^{-ik_3L}r_3 & e^{-ik_4L}r_4 & e^{-ik_5L}r_5 & e^{-ik_6L}r_6 \\ e^{-ik_1L} & e^{-ik_2L} & e^{-ik_3L} & e^{-ik_4L} & e^{-ik_5L} & e^{-ik_6L} \\ -ik_1e^{-ik_1L} & -ik_2e^{-ik_2L} & -ik_3e^{-ik_3L} & -ik_4e^{-ik_4L} & -ik_5e^{-ik_5L} & -ik_6e^{-ik_6L} \end{bmatrix},$$

Assuming general solutions of the type

$$W(x,\omega)=\boldsymbol{N}_w(x,\omega)\boldsymbol{H}_{BP}^{-1}(\omega), \qquad U(x,\omega)=\boldsymbol{N}_u(x,\omega)\boldsymbol{d}, \tag{18}$$

where the shape functions are given by

$$\boldsymbol{N}_w(x,\omega)=\boldsymbol{e}(x,\omega)\boldsymbol{H}_{BP}^{-1}(\omega), \qquad \boldsymbol{N}_u(x,\omega)=\boldsymbol{e}(x,\omega)\boldsymbol{R}\boldsymbol{H}_{BP}^{-1}(\omega), \tag{19}$$

Relating the general solution to the equation of motion and applying Hamilton's principle, we arrive at the following spectral element equation

$$\boldsymbol{S}_{BP}(\omega)\boldsymbol{d}=\boldsymbol{f}(\omega), \tag{20}$$

and replacing the dynamic shape functions into Eq. (20) gives

$$\boldsymbol{S}_{BP}(\omega)=\boldsymbol{H}_{BP}^{-T}(\omega)\boldsymbol{D}(\omega)\boldsymbol{H}_{BP}^{-1}(\omega), \tag{21}$$

where

$$\boldsymbol{D}(\omega)=-EA\boldsymbol{RKEKR}+EI\boldsymbol{K^2EK^2}-i\beta(\boldsymbol{K^2EKR}+\boldsymbol{RKEK^2})-\omega^2[\rho A(\boldsymbol{E}+\boldsymbol{RER})+i\alpha(\boldsymbol{KER}+\boldsymbol{REK})-\gamma KEK]+i\omega[cA(\boldsymbol{E}+\boldsymbol{RER})-c_1\boldsymbol{KEK}+ic_4(\boldsymbol{KER}+\boldsymbol{REK})]-F\boldsymbol{RER},$$

with

$$\boldsymbol{K}=diag[k_j], \qquad \boldsymbol{K^2}=diag[k_j^2], \qquad \boldsymbol{E}(\omega)=\int_0^L \boldsymbol{e}^T(x,\omega)\boldsymbol{e}(x,\omega)dx,$$

2.3 Spectral element shunt control

The mathematical representation of connecting an electrical shunt circuit to a piezoelectric represents the energy relation with mechanical deformation. The equation of beam-piezo movement with electrical shunt circuit is given by

$$\begin{aligned} &EIw''''+\rho A\ddot{w}+cA\dot{w}+\Gamma V=-\alpha\ddot{u}_b'+\beta u'''+\gamma\ddot{w}''+c_1\dot{w}''-c_4\dot{u}_b'+Fw''+p(x,t)\\ &EAu_b''-\rho A\ddot{u}_b-cA\dot{u}_b+\Gamma V=-\alpha\ddot{w}'+\beta w'''-c_4\dot{w}'-\tau(x,t),\\ &E\Gamma\dot{x}+C_p^T\dot{V}=I, \end{aligned} \tag{22}$$

where I is current, V is the voltage, C_p^T is the piezoelectric capacitance, Γ is the coupling term, defined by the following relationships

$$V=-Z_{eq}I, \qquad C_p^T=A(C_{11}^D-h_{31}^2/\beta_{33}^S), \qquad \Gamma=A(C_{11}^D-h_{31}^2/\beta_{33}^S)/l \tag{23}$$

where Z_{eq} is the electrical impedance of the shunt circuit. The resonant type electrical shunt circuit with resistance and inductance connected in series, the following impedance is generated

$$Z_{eq}=\frac{R+i\omega L}{\left(1-\omega^2LC_p^T\right)+i\omega RC_p^T} \tag{24}$$

Eq. (22) can be particularized to a harmonic motion and converted to the frequency domain. Thus, the corresponding harmonic motion assumption for generalized force and current is given by

$$\begin{aligned} &\boldsymbol{S}_{BP}(\omega)\boldsymbol{d} - \boldsymbol{S}_{SH}(\omega)V(\omega) = \boldsymbol{f}(\omega), \\ &i\omega\boldsymbol{S}_{SH}(\omega)\boldsymbol{d} + i\omega\, C_p V(\omega) = I(\omega), \end{aligned} \tag{25}$$

Rearranging the equation of motion in terms of the piezo-beam and shunt circuit spectral element matrices, one can obtain:

$$[\boldsymbol{S}_{BP}(\omega) + \boldsymbol{S}_{SH}(\omega)]\boldsymbol{d} = \boldsymbol{f}(\omega), \tag{26}$$

where

$$\boldsymbol{S}_{sh}(\omega) = \begin{bmatrix} \boldsymbol{N}_e(x_0,\omega) \\ 0 \\ -\boldsymbol{M}_e\,(x_0,\omega) \\ -\boldsymbol{N}_e(x_0,\omega) \\ 0 \\ \boldsymbol{M}_e(x_0,\omega) \end{bmatrix}$$

with

$$\boldsymbol{N}_e = \frac{k_{31}^2 i\omega Z_{eq} b d_{31} E_p}{1 + i\omega C_p^T Z_{eq}}, \qquad \boldsymbol{M}_e = \frac{k_{31}^2 i\omega Z_{eq} h b d_{31} E_p}{2 + 2i\omega C_p^T Z_{eq}}$$

Once the matrices of the spectral elements $\boldsymbol{S}_B(\omega)$, $\boldsymbol{S}_{BP}(\omega)$ and $\boldsymbol{S}_{SH}(\omega)$ are defined, it is possible to obtain the global matrix by assembling the elements. This procedure is similar to the one used in the Finite Element Method. Therefore, the global equation can be written so that

$$\boldsymbol{S}_g(\omega)\boldsymbol{d}_g(\omega) = \boldsymbol{f}_g(\omega), \tag{27}$$

Where the subscript g indicates the global components.

3. TRANSFER MATRIX METHOD

The Transfer Matrix Method (TMM) combined with the SEM results in a dynamic analysis called the Spectral Transfer Matrix Method (STMM) (Lee, 2009). In this method, the spectral element modelling of the κ-th lattice cell can be assembling the spectral element models of all face members in global coordinates of the form

$$\begin{bmatrix} \boldsymbol{S}_{g_{\mathrm{lr}}}(\omega) & \boldsymbol{S}_{g_{lr}}(\omega) \\ \boldsymbol{S}_{g_{rl}}(\omega) & \boldsymbol{S}_{g_{rr}}(\omega) \end{bmatrix}_{\kappa} \begin{Bmatrix} \boldsymbol{d}_{g_l} \\ \boldsymbol{d}_{g_r} \end{Bmatrix}_{\kappa} = \begin{Bmatrix} \boldsymbol{f}_{g_l} \\ \boldsymbol{f}_{g_r} \end{Bmatrix}_{\kappa} \tag{28}$$

where l and r correspond to the nodes of the left and right sections of the cell, respectively. The Eq. (28) can be transformed relating the left and right components as

$$\begin{Bmatrix} \boldsymbol{d}_{g_r} \\ \boldsymbol{f}_{g_r} \end{Bmatrix}_{\kappa} \begin{bmatrix} -\boldsymbol{S}_{g_{lr}}^{-1}\boldsymbol{S}_{ll} & -\boldsymbol{S}_{g_{lr}}^{-1} \\ \boldsymbol{S}_{g_{rl}} - \boldsymbol{S}_{g_{rr}}\boldsymbol{S}_{g_{lr}}^{-1}\boldsymbol{S}_{g_{ll}} & -\boldsymbol{S}_{g_{rr}}\boldsymbol{S}_{g_{lr}}^{-1} \end{bmatrix}_{\kappa} = \begin{Bmatrix} \boldsymbol{d}_{g_l} \\ \boldsymbol{f}_{g_l} \end{Bmatrix}_{\kappa} \tag{29}$$

or, simply $\boldsymbol{P}_{\kappa Rr} = \boldsymbol{t}_k(\omega)\boldsymbol{P}_{\kappa l}$, where

$$\boldsymbol{P}_{\kappa r} = \begin{Bmatrix} \boldsymbol{d}_{g_r} \\ \boldsymbol{f}_{g_r} \end{Bmatrix}_{\kappa}, \qquad \boldsymbol{P}_{\kappa l} = \begin{Bmatrix} \boldsymbol{d}_{g_l} \\ \boldsymbol{f}_{g_l} \end{Bmatrix}_{\kappa}, \qquad \boldsymbol{t}_{\kappa}(\omega) = \begin{bmatrix} -\boldsymbol{S}_{g_{lr}}^{-1}\boldsymbol{S}_{ll} & -\boldsymbol{S}_{g_{lr}}^{-1} \\ \boldsymbol{S}_{g_{rl}} - \boldsymbol{S}_{g_{rr}}\boldsymbol{S}_{g_{lr}}^{-1}\boldsymbol{S}_{g_{ll}} & -\boldsymbol{S}_{g_{rr}}\boldsymbol{S}_{g_{lr}}^{-1} \end{bmatrix}_{\kappa}$$

The matrix $\boldsymbol{t}_{\kappa}(\omega)$ is the transfer matrix derived from the spectral element model for the k-th lattice cell, and it relates the state-vector $\boldsymbol{P}_{\kappa l}$ (left) to the state-vector $\boldsymbol{P}_{\kappa r}$ (output). Therefore, the state vectors satisfy

$$\boldsymbol{P}_{(\kappa-1)R} = \boldsymbol{P}_{kl} \quad (\kappa = 1, 2, \ldots N) \tag{30}$$

If the substructure is a periodic lattice structure with N lattice cells identical, each network cell will have the transfer matrix with $\boldsymbol{t}_1(\omega) = \boldsymbol{t}_2(\omega) = \ldots = \boldsymbol{t}_N(\omega) = \boldsymbol{t}(\omega)$. Therefore, the state vector $\boldsymbol{P}_{kR}r$ at the far right of a network can be related to the state vector $\boldsymbol{P}_{kL}$ at its left end to a substructure with

$$\boldsymbol{P}_{Nr} = \boldsymbol{T}(\omega)\boldsymbol{P}_{1l} \tag{31}$$

where $\boldsymbol{T}(\omega) = \boldsymbol{t}_N(\omega)\boldsymbol{t}_{N-1}(\omega)\ldots\boldsymbol{t}_2(\omega)\boldsymbol{t}_1(\omega)$ is the global transfer matrix for all substructures of the network. If the network substructure corresponds to a periodic structure consisting of N cells identical to the network, the global transfer matrix can be further simplified with

$$\boldsymbol{P}_{Nr}\boldsymbol{e}^{\mu} = \boldsymbol{T}(\omega)\boldsymbol{P}_{1l} \tag{32}$$

The Eq. (32) obeys Floquet-Bloch's theorem for wave propagation in a periodic system. The term $\mu = -ikL$ is the attenuation constant, where k is the wavenumber. Transfer matrix approach does not require prior knowledge of the wave solutions or exact shape functions of the problem. However, if all eigenvectors of the $\boldsymbol{S}_g(\omega)$ matrix are linear, the wavenumbers and waveforms can be calculated (Zhong and Williams, 1995).

4. NUMERICAL ANALYSIS

In this article, the properties and geometries for the beam with piezoelectric layer followed the work of Lee and Kim (2000) to validate the results. Table 1 demonstrates the properties of the smart beam structure.

Table 1. Experimental results for flexural properties of CFRC-4HS and CFRC-TWILL composites. Span/depth ratio = 35:1. Average results of 7 specimens.

Properties	Beam	Piezo
Length [mm]	261.6	18.68
Width [mm]	12.7	12.7
Thickness [mm]	2.286	0.762
Young's Modulus [GPa]	71	64.9
Density [kg/m^3]	2700	7600
Dielectric constant [m/V]	-175e^{-12}	
Coupling coefficient	0.31	
Piezoelectric capacitance [nF]	200	

The simulation was performed in MATLAB software, presenting a series resistive-inductive shunt circuit configuration with values of resistance $R = 33\ \Omega$ and inductance $L = 0.1516\ H$ for a frequency tuned at 919 Hz, which is related to the third vibration mode of the beam. The circuit's impedance and topography are shown in Figure 2.

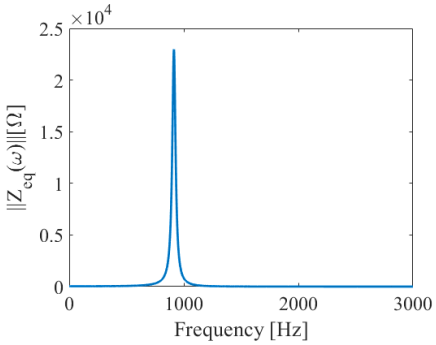

(a)

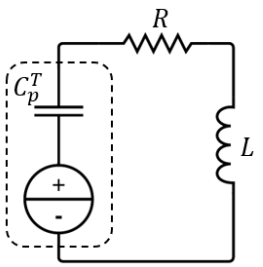

(b)

Figure 2. Resistive-inductive shunt circuit: a) Electrical impedance; b) Circuit topography.

Figure 3 (a-d) shows the Frequency Response Functions (FRF) of the smart material beam in the free-free boundary condition. The vibrational analysis is performed considering a unit impulse at the right edge of the structure, at the penultimate node, and measurements are taken at the same point (orange line) and the left edge (blue line). Comparing the number of piezo to the beam reveals a trend of attenuation and the formation of a bandgap. The bandgap effect happens at the design frequency of the shunt circuit performing the vibrational control via the RL piezo-shunt, which shows to be feasible for the generation of band gaps.

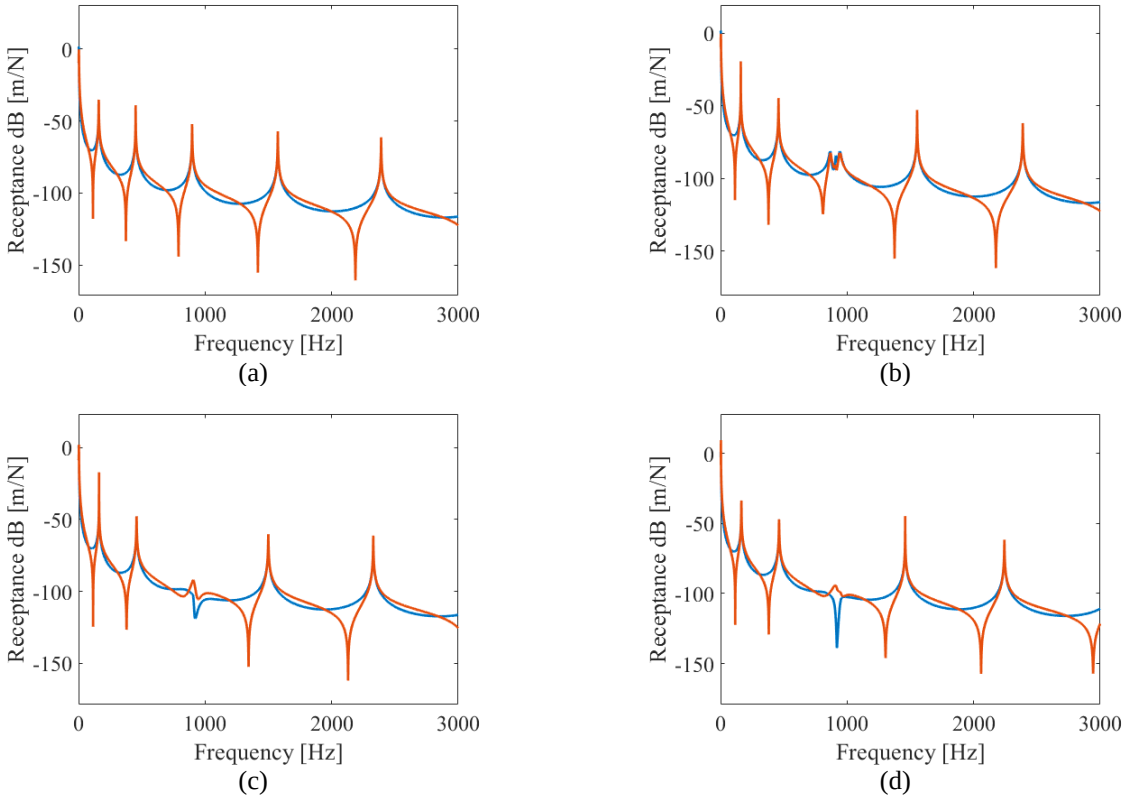

Figure 3. FRF measured at the penultimate node (orange line) and on the second node (blue line) of smart material beam in coupling configurations with: a) 4 piezo's shorted; b) 4 piezo's with resonant shunt; c) 5 piezo's with resonant shunt; d) 7 piezo's with resonant shunt.

In Figure 3 (b-d), by assuming four piezo sensors and shunt circuits, there is an attenuation in the tuned frequency at the third mode shape of the receptance response. As the use of piezo-shunts increased, a bandgap appears. It is well seen at the receptance response obtained on the opposite side of the excitation (blue line). Similar to the coupling configurations adopted in Figure 3, the dispersion diagrams of the smart beam coupled with four piezo's shorted and 4 to 7 piezo's with resonant shunt are shown in Figure 4 (a-d).

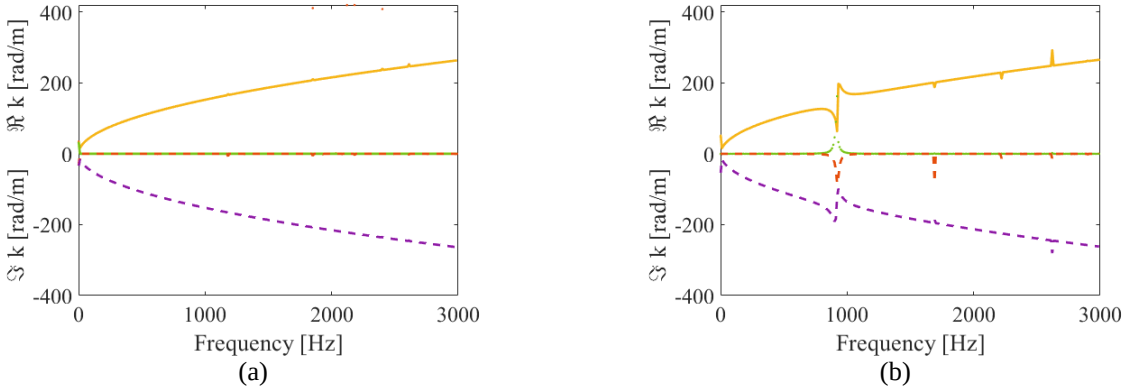

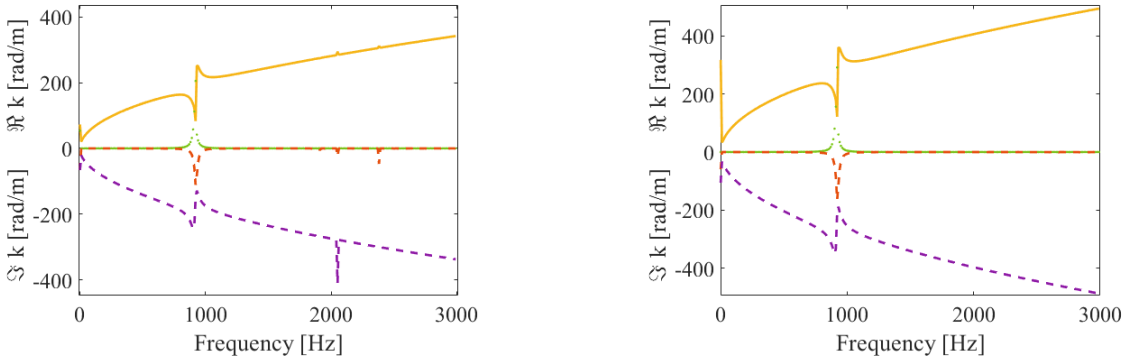

Figure 4. Dispersion diagram showing the transverse (yellow and purple lines) and longitudinal (orange and green lines) waves of smart material in coupling configurations with a) 4 piezo's shorted; b) 4 piezo's with resonant shunt; c) 5 piezo's with resonant shunt; d) 7 piezo's with the resonant shunt.

The attenuation effect appears at the tuned frequency range at the real and imaginary parts of the wavenumbers. The smart beam's flexural waves are printed in yellow and purple lines, and the waves are corresponding to the circuit shunt in green and orange lines. A pattern of attenuation can be observed in the wave set of the smart material beam at the tuned frequency. Therefore, it is understood that the periodicity and the number of piezo-shunt couplings to the beam influence the wave attenuation. However, the change in wavenumber could already be captured with just four piezo-shunt patches, as no significant change happened with the increase in the number of sensors.

5. COMMENTS AND FINAL REMARKS

In summary, in this article, resistive-inductive piezo-shunt is a passive control capable of generating the bandgap effect. The vibrational behavior demonstrated by the FRFs proves the attenuation and stopping effects of vibration arising from the shunt configuration discussed here. Likewise, wave propagations shown in the scatter diagrams also demonstrate the effects of attenuation and stopping of vibration. This paper showed a study of a shunt circuit well used in the literature. Several combinations of circuits can be used to control or impose some effect on vibrations and wave propagation and the generation of the bandgap effect.

6. REFERENCES

Airoldi, L., and Ruzzene, M., 2011. "Design of tunable acoustic metamaterials through periodic arrays of resonant shunted piezo". *New Journal of Physics*, 13(11), Nov., p. 113010.

Barbosa B., Machado, M., 2019. "Analysis of vibration attenuation in a beam coupled with a piezoelectric in shunt configuration using the spectral element method". In *25th International Congress of Mechanical Engineering - COBEM*, Uberlândia, Brazil.

Chen, Y. Y. et al., 2014. "Band gap control in an active elastic metamaterial with negative capacitance piezoelectric shunting". *Journal of Vibration and Acoustics*, v. 136.

Doyle, J. F., 1997. Wave Propagation in Structures, Springer Verlag, New York.

Forward, R. L., 1979. "Electronic damping of vibrations in optical structures". *J. Appl. Opt.*18(5), p. 690–697.

Gripp, J. A. B., and Rade, D. A., 2018. "Vibration and noise control using shunted piezoelectric transducers: A review". *Mechanical Systems and Signal Processing*, 112, Nov., pp. 359–383.

Jaffe, B. et al., 1971. Engineering vibration. 2. ed. upper saddle river: Prentice-hall. Piezoelectric Ceramics. New York: Academic Press.

Lee, U., 2009. Spectral element method in structural dynamics. Singapore, Wiley.

Lee, U., and Kim, J., 2000. "Dynamics of elastic-piezoelectric two-layer beams using spectral element method". *International Journal of Solids and Structures*, 37, pp. 4403–4417.

Leo, D. J., 2007. Engineering analysis of smart material systems. John Wiley and Sons, New Jersey, p. 1–7.

Machado, M. R., Fabro, A. T., and Moura, B. B., 2019. "Flexural waves propagation in piezoelectric metamaterial beam". *15th International Conference Dynamical Systems - Theory and Applications*, Lodz, Poland.

Machado, M. R., Fabro, A. T., and Moura, B. B., 2019. "Spectral element approach for flexural waves control in smart material beam with single and multiple resonant impedance shunt circuit". *Journal of Computational and Nonlinear Dynamics*.

Moura, B. B. et al., 2020. "Vibration and wave propagation control in a smart metamaterial beam with periodic arrays of shunted piezoelectric patches". *49th International Congress and Exposition on Noise Control Engineering, INTER-NOISE*, Seoul, Korea.

Moura, B. B. and Machado, M. M., 2021. "Vibration control using piezoelectric connected with shunts circuits". *14th World Congress on Computational Mechanics (WCCM), ECCOMAS Congress*, Virtual Congress.

Santana, D. C. et al., 2003. “Estudo de técnicas de controle de vibração empregando piezocerâmicas combinadas com circuitos shunt”. *13º POSMEC - Simpósio do Programa de Pós-Graduação em Engenharia Mecânica*. FEMEC/UFU, Uberlândia, Brazil.

Zhong, W. and Williams, F., 1995. "On the direct solution of wave propagation for repetitive structures". *Journal of Sound and Vibration*, vol. 181, no. 3, pp. 485-501.

7. RESPONSIBILITY NOTICE

The author(s) is (are) the only responsible for the printed material included in this paper.